Revealing Excitonic Complexes in Monolayer WS_2 on Talc Dielectric

Gabriela Augusta Prando,[1] Marion E. Severijnen,[2,3] Ingrid D. Barcelos,[4] Uli Zeitler,[2,3] Peter C. M. Christianen,[2,3] Freddie Withers,[5] and Yara Galvão Gobato[1,2,*]

[1] *Physics Department, Federal University of São Carlos, São Carlos, Brazil*
[2] *High Field Magnet Laboratory (HFML - EMFL), Radboud University, 6525 ED, Nijmegen, Netherlands*
[3] *Institute for Molecules and Materials, Radboud University, 6525 AJ, Nijmegen, Netherlands*
[4] *Brazilian Synchrotron Light Laboratory (LNLS), Brazilian Center for Research in Energy and Materials (CNPEM), 13083-970 Campinas, SP, Brazil*
[5] *College of Engineering, Mathematics and Physical Sciences, University of Exeter, Exeter EX4 4QF, United Kingdom*

(Received 15 August 2021; revised 16 November 2021; accepted 17 November 2021; published 23 December 2021)

We report on a detailed study of low-temperature photoluminescence (PL) and magnetophotoluminescence under perpendicular magnetic fields (up to 30 T) and circularly polarized excitation on high-quality monolayer (ML) WS_2 on a thick layer (120 nm) of talc dielectric. Remarkably, we obtained high-quality samples without any evidence of localized exciton emission at low temperature and a PL linewidth comparable to that of WS_2/h-BN samples. As a consequence, we observe well-resolved emission peaks at low temperature due to the formation of excitonic complexes, including a dark-trion (DT) state and phonon replicas of the DT without the application of an in-plane magnetic field. The nature of the emission peaks, the magnetic field dependence of the degree of polarization, and g factors are discussed in detail and compared with the corresponding results obtained for h-BN encapsulated transition-metal dichalcogenide (TMD) samples. We observe that under σ^+-polarized excitation the sign of the circular polarization of biexcitons is reversed under higher magnetic fields. In addition, the dark-trion polarization increases considerably with increasing perpendicular magnetic field, demonstrating different behavior compared with previous studies of dark trions on monolayer WSe_2. Our results suggest that talc is indeed a promising layered material for the surface protection of ML TMDs and to explore fundamental physics in view of applications in optoelectronic devices.

DOI: 10.1103/PhysRevApplied.16.064055

I. INTRODUCTION

Two-dimensional (2D) transition-metal dichalcogenides (TMDs) are very attractive systems for studying the physics of strong spin-valley coupling and excitonic effects [1,2]. The strong Coulomb interaction in monolayer (ML) TMDs results in the formation of different excitonic complexes involving electrons and holes in the conduction (CB) and valence (VB) bands of the K and K' valleys [1–10]. Several dark- and bright-exciton complexes were recently unveiled due to the improved optical quality of ML TMDs, as a result of hexagonal boron nitride (h-BN) encapsulation, which reduces considerably the linewidth of the photoluminescence (PL) emission and increases its intensity [4,11]. Dark excitonic complexes are not allowed to undergo radiative recombination due to spin conservation and/or momentum selection rules [5,7,12–14]. Dark excitons are of particular interest because of their long lifetimes and possibly long valley-coherence times [5,15]. Furthermore, despite intense recent investigations of the fine structure of bright- and dark-exciton complexes in ML TMDs, the detailed nature of the lower-energy emission peaks of monolayer TMDs, such as WS_2, is still unresolved. Most of the magneto-PL studies have been performed on ML TMDs [16] on SiO_2 or on MLs encapsulated by h-BN, the latter of which shows high-quality optical properties of significant relevance for future device applications and for fundamental physics investigations. However, it is also interesting to develop alternative layered dielectric and atomically flat substrates, to circumvent the complex growth requirements for high-quality h-BN. Moreover, from a fundamental point of view, studies on the impact of different dielectric materials on doping and the magneto-optical properties of monolayer TMDs are scarce.

Talc [chemical formula $Mg_3Si_4O_{10}(OH)_2$] is an abundant van der Waals layered magnesium silicate mineral [17], the crystalline structure of which contains three octahedral Mg positions per four tetrahedral Si positions. It is

*yara@df.ufscar.br

an insulator with a high band gap (approximately 5.3 eV) [17] and a high dielectric constant of up to nine, depending on its doping [18,19]. Talc has a high thermal stability [18] and is chemically inert [18,20]. In contrast to SiO_2, talc is a genuine two-dimensional (2D) natural silicate dielectric material, which possesses atomically flat surfaces [18,20]. Previous reports have demonstrated the use of talc within graphene transistors and the obtained results compare well with those obtained using *h*-BN substrates [18]. These properties are promising for possible applications as an insulating medium compatible with atomically thin *p*-*n* junctions and field-effect transistors for ultracompact devices [18,20]. Therefore, talc has excellent properties, making it a potential candidate as a low-cost dielectric material. More recently, it was observed that MoS_2-talc samples with a talc thickness of 30 nm presented an enhancement in the PL intensity and a reduced PL linewidth (40–45 meV, depending on the laser position) at 300 K, as compared to MoS_2/SiO_2 (50–80 meV) [21]. It is also shown that talc is a promising dielectric for 2D devices [22]. However, there are no previous detailed studies of PL and magneto-PL of ML TMD-talc at low temperatures. Since the PL linewidths at low temperature usually reflect homogeneous and/or inhomogeneous contributions to the PL spectrum, such experiments are essential to probe the ultimate optical quality of ML TMDs.

Here, we investigate the optical properties of ML WS_2 deposited on a thick talc layer. Our findings demonstrate that the use of a few layers of talc results in high-quality doped WS_2 MLs with a reduced photoluminescence linewidth and interesting valley properties. We probe the optical properties of ML WS_2 on talc at low temperature and magnetic fields up to 30 T. We observe several emission peaks due to the formation of different bright- and dark-exciton complexes with different *g* factors. In general, our results show that talc is a promising layered material to explore fundamental physics and for possible application in optoelectronic devices based on high-quality doped TMDs.

II. SAMPLE PREPARATION AND EXPERIMENTAL METHODS

Our samples are prepared by conventional all-dry transfer techniques and consist of a ML of WS_2 (bulk crystals from HQ Graphene) on a layer of talc (natural crystal from a mine of Ouro Preto, Minas Gerais, Brazil). The talc layers are exfoliated with Scotch tape and placed onto SiO_2/Si substrates. The WS_2 MLs are first exfoliated with Scotch tape and later exfoliated again on a polydimethylsiloxane stamp and placed on a glass slide for inspection with an optical microscope.

For the experiments, the ML WS_2 sample is mounted on Attocube piezoelectric *x*-*y*-*z* translation stages to control the sample position with submicron precision. The sample is cooled by helium exchange gas (temperatures around 4.2 K) within a liquid-helium bath cryostat, placed in a Florida-Bitter magnet with a maximum magnetic field strength of $B = 30$ *T*. The PL measurements are performed using a continuous-wave green laser with a photon energy of 2.33 eV, which is focused by an Attocube objective ($40\times$, numerical aperture $NA = 0.55$) to a spot size of about 3 μm. The resultant PL signal is collected by the same objective and measured by a Princeton spectrometer (Acton SpectraPro-300i) equipped with a liquid-nitrogen-cooled charge coupled device (PyLoN from Princeton Instruments). Circular polarization is controlled independently for the excitation and detection beams by using appropriate optics, consisting of quarter-wave plates and linear polarizers. Light propagation is parallel to the direction of the magnetic field (Faraday configuration).

III. RESULTS AND DISCUSSION

Figure 1 shows schematically the configurations of the different excitonic states for *n*-doped monolayer WS_2: the bright neutral exciton (X), dark neutral exciton (DX), bright intervalley negative trion (Tt), bright intravalley negative trion (Ts), negative dark trion (DT), biexciton (XX), and charged biexciton (XX^-). Particularly, the DX at the *K* valley has an electron in the lowest CB level and a hole in the highest VB level. A DT can be formed by an exciton in the *K* valley and an extra electron in the K' valley. Furthermore, strong Coulomb coupling gives rise to strong exciton-exciton interactions, resulting in the formation of XX, formed by bright and dark excitons in the *K* and K' valleys. Similarly, XX^- can be formed with an extra electron in the *K* valley [5]. Recently, it was reported that the DT configuration results in two different recombination channels [12,23], depending on the electron involved in the emission process itself. One emission pathway (TD) involves recombination of an electron-hole pair from the same *K* or K' point via an intravalley spin-forbidden transition [12]. The other transition (TI) involves recombination of an electron and a hole from different valleys through an intervalley momentum-forbidden transition [12]. The lower-energy transition (TI) was recently observed at zero magnetic field and the higher-energy transition (TD) was observed under an applied parallel magnetic field (Voigt configuration) [12]. The energy separation between these two dark trion transitions is reported to be on the order of 530 μeV for ML WS_2 and the reported *g*-factor values for the TD and TI transitions are found to be equal to -8.9 and -13.7, respectively [12].

Figure 2(a) shows an optical microscopy image of a ML WS_2-talc sample, together with an atomic force microscopy (AFM) image of the talc layer. The AFM results demonstrate that the talc layer has a thickness of about 120 nm and provides an atomically flat surface [root-mean-square (rms) roughness, $R_{rms} \leq 0.35$ nm],

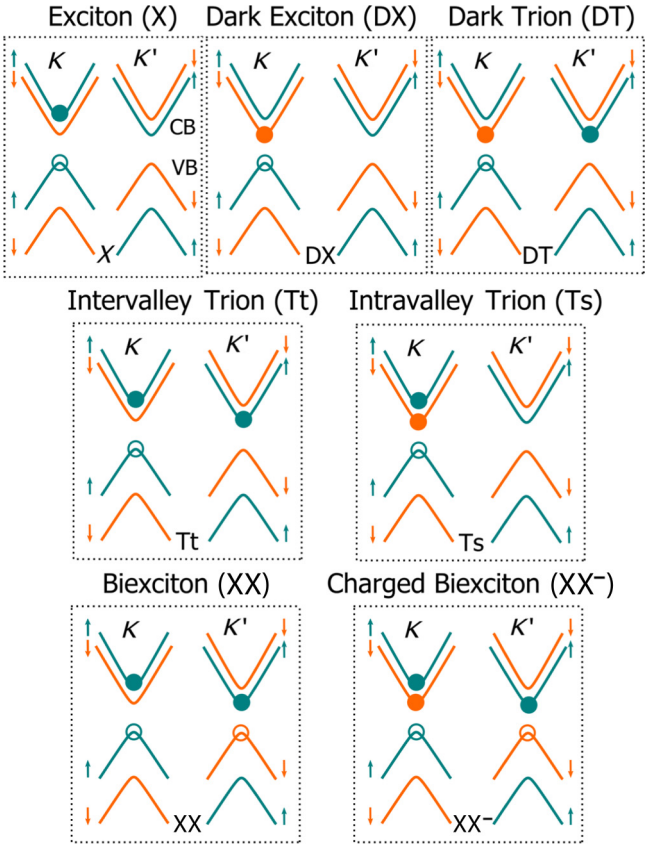

FIG. 1. Schematic configurations of expected bright or dark excitons and trions, XX, and XX^- at the K and K' valleys for an n-doped monolayer WS_2. Arrows and colors indicate spin directions in the VB and CB. X and T emit circularly polarized light in the out-of-plane direction; DX and DT emit vertically polarized light in the in-plane direction.

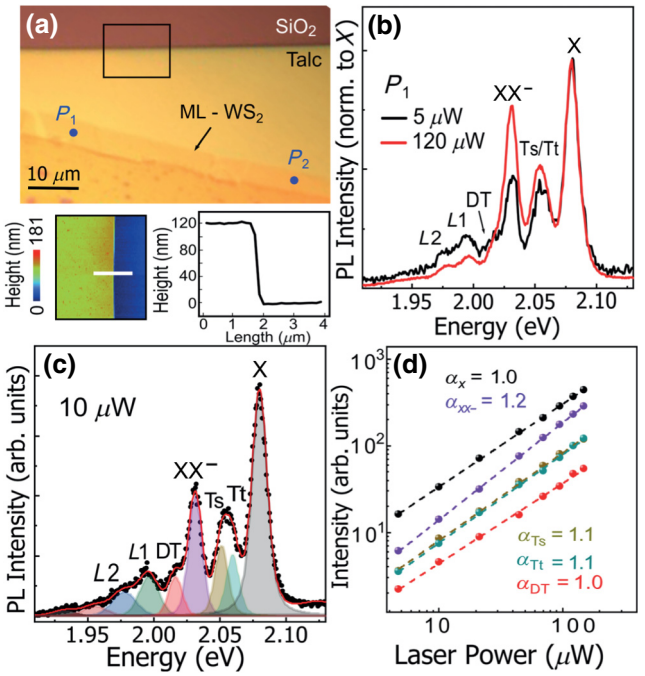

FIG. 2. (a) Optical microscope and AFM images of the WS_2-talc ML sample. (b) Typical PL spectra for position $P1$ for two selected laser powers (5 and 120 μW) at 4.5 K (c) Typical fitting of the PL spectrum at zero magnetic field. (d) Double-logarithmic plot of integrated intensities of different excitonic peaks as a function of laser power.

which is an important property to obtain high-quality samples. Figure 2(b) shows typical low-temperature (4.2 K) PL spectra for two different laser powers (5 and 120 μW) for the position labeled $P1$. The PL spectra are normalized to the intensity of the X peak. The PL spectra of the WS_2-talc sample are stable [22], and no photodoping effect [24] is observed. Figure S1 within the Supplemental Material [25] shows in more detail the spectra for different laser powers. Similar results are obtained for different laser positions on the sample (Fig. S2 within the Supplemental Material [25]). The PL spectrum is composed of several emission peaks, associated with the emission of different excitonic complexes. Specifically, we can identify the X emission at 2.086 eV and negative-trion recombination around an energy of 2.056 eV. The full width at half maximum (FWHM) of the exciton peak is in the order of 10 meV at 4.5 K (approximately equals 26–30 meV at 300 K, depending on the laser position) showing that talc is a promising dielectric to separate monolayer TMD from the SiO_2 substrate. Indeed, this value is much lower than the reported value of ML WS_2 on SiO_2, which is around 20 meV (approximately equals 35–50 meV at 300 K) [9,24,26], and comparable that of to ML WS_2 on h-BN, which is around 10 meV [27,28]. Our results also show improved sample quality using a thicker talc layer (120 nm) compared with previous work on MoS_2. However, it is not easy to compare the results of FWHM for different TMD materials. In addition, it should be mentioned that the different values of the FWHM at 300 K for samples with different talc thicknesses could be due to different sample inhomogeneity introduced into the exfoliation and transfer method or due to different doping levels. Actually, typical impurities in our talc crystals are Fe and Al, which are known to result in p doping of graphene [18]. It is shown that Fe or Al impurities occupy Si sites in talc and act as acceptors [18]. Therefore, these impurities remove electrons from the graphene layer, resulting in a p-type doping effect [18]. A similar result is expected for ML TMD-talc heterostructures. Actually, we have observed recently that TMD-talc FET devices with a layer thickness below 40 nm are slightly more p type than MoS_2 and $MoSe_2$ transistors on h-BN or SiO_2 dielectrics [22]. We anticipate that the FWHM of the X emission of WS_2-talc can be further reduced by using an appropriate thermal treatment, such as the standard procedures used for h-BN-encapsulated TMD monolayers [29].

The trion peak exhibits a clear asymmetry, the appearance of which depends on the laser position on the sample. This observation strongly suggests that the WS_2-talc ML is *n*-doped, such that the trion emission is composed of two different bright negatively charged species, i.e., intralayer and interlayer trions, as illustrated in Fig. 1. In our case, the bright-trion PL peak consists of a singlet (Ts) peak, around 2.053 eV and a triplet (Tt) peak around 2.060 eV, split by the Coulomb exchange interaction [5,26,30] (Fig. 1). The energy separation between the Tt and Ts peaks is in the order of 7 meV, similar to the trion splitting observed for WS_2 on *h*-BN [31,32]. The intensity of the total trion band for the two laser powers (5 and 120 μW) is approximately equal to the exciton intensity [Fig. 2(b)]. The laser-power dependencies of both the X and trion PL intensities, obtained by fitting the spectra using Voigt functions [Fig. 2(c)], shows a linear relationship dependence with laser power [Fig. 2(d)]. Using $I \propto P^{\alpha}$, where I is the integrated PL intensity and P is the laser power, we obtain $\alpha = 1.0$ for the exciton peak and $\alpha = 1.1$ for the trion peak. In contrast, the peak at around 2.031 eV shows superlinear behavior as a function of laser power [5,33] ($\alpha = 1.2$). We attribute this peak to the emission of XX^-, giving a binding energy of about 55 meV, which is consistent with previous reports in the literature [5,24,33–35]. It is shown that the emission of neutral biexcitons in $MoSe_2$, WSe_2, and WS_2 MLs is located at an energy in between the exciton and trion PL peaks, with a typical binding energy of around 20 meV, in agreement with theoretical predictions [5]. The unambiguous identification of both neutral and charged XX transitions was recently reported through experiments using electrostatic gating, ranging from hole to electron doping [5]. Therefore, the energy position and laser-power dependence of the 2.031 eV peak confirm its origin to be that of the emission of XX^- [5,24,33,35–37]. While a nearly quadratic power law is expected for full thermal equilibrium between neutral exciton and biexcitons, values smaller than two, like we observe, were reported recently in other TMD MLs [5,33–35,37].

At lower laser powers [Figs. 2(b) and 2(c)], we observe clearly an additional emission peak at around 2.016 eV, which is attributed to DT emission [5]. Figure S1 within the Supplemental Material [25] shows more details on the DT emission for different laser powers. As mentioned above, transitions of these dark states are optically forbidden for in-plane polarized light [5], i.e., in the backscattering-geometry scheme we use. However, it is shown that an objective with a large numerical aperture, as used in our experiments, permits the detection of dark-exciton emission in ML TMDs [5]. In addition, emission of dark-exciton states can also be caused by disorder or strain from the talc substrate, which can break the optical selection rules. Finally, we observe additional lower-intensity emission peaks at lower energies, labeled $L1$ and $L2$ in Figs. 2(b) and 2(c). We note that, for this position, $P1$, the energy separation of these peaks from the DT peak is about 20 meV for $L1$ and about 38 meV for $L2$, which are very close to the phonon energies in ML WS_2 [12]. Therefore, a possible cause for the origin of these peaks could be the occurrence of phonon replicas [38] of dark trions.

Figure 3 presents the polarization-resolved magneto-PL spectra and corresponding false-color PL-intensity plots, as a function of magnetic field for position $P2$ using circularly polarized excitation. Figure S3 within the Supplemental Material [25] shows similar magneto-PL results for position $P1$.

With increasing magnetic field, we observed blue- and redshifts, respectively, for σ^-- and σ^+-circularly polarized PL, as expected [37,39–45]. We fit the magneto-PL spectra with a set of eight Voigt functions, and Fig. 4(a) shows the PL peak positions, E, for σ^-- and σ^+-circularly polarized emission, given by $E = E_0 \pm \frac{1}{2} g \mu_B B$, where E_0 is the energy of each species at zero magnetic field, g is the g factor of each excitonic complex, and $\mu_B \sim 58\ \mu eV/T$ is the Bohr magneton. Figure 4(b) displays the corresponding magnetic-field-induced valley splittings. To extract the g factors, we perform linear fittings of the Zeeman splittings, ΔE, using

$$\Delta E = E^{\sigma+} - E^{\sigma-} = g \mu_B B. \tag{1}$$

The fitting results are indicated by the solid lines in Fig. 4(b). We obtain $g_X \approx -3.6$ for the exciton, $g_{Ts} = g_{Tt} \approx -3.9$ for the singlet and triplet trion states, $g_{XX-} \approx -4.3$ for the charged biexciton, and $g_{DT} \approx -9.3$ for the dark trions. The obtained values of the g factors for the bright excitons, trions, and charged biexciton are consistent with previous values reported in the literature [5,12,31,33,45–47]. Furthermore, the g factor of the spin-forbidden dark-trion peak is very similar to the values obtained for ML WSe_2 [5,6] and for the TD peak under a tilted magnetic field in ML WS_2 [2,6].

Figure 4(c) shows the magnetic field dependence of the degree of circular polarization of each species, defined by $P = (I_{\sigma+} - I_{\sigma-})/(I_{\sigma+} + I_{\sigma-})$. It is important to note that, in our experiments, we use circularly polarized excitation. Therefore, we observe that the polarization of the X emission is constant (around 15%) with varying magnetic field. This constant exciton polarization can be understood as a result of the valley selection effect under circularly polarized excitation, which is field independent for the W-based ML [43]. The trion degrees of polarization are also consistent with those reported in previous studies [16,31]. For the singlet trions, we observe a rather low value of polarization degree with small changes of increasing magnetic field, with indications of a sign reversal at finite fields, in agreement with previous results [31]. For the triplet trions, we observe a field-dependent, yet always positive, polarization degree. However, it is difficult to provide a detailed discussion of the field dependence of trion polarization, as

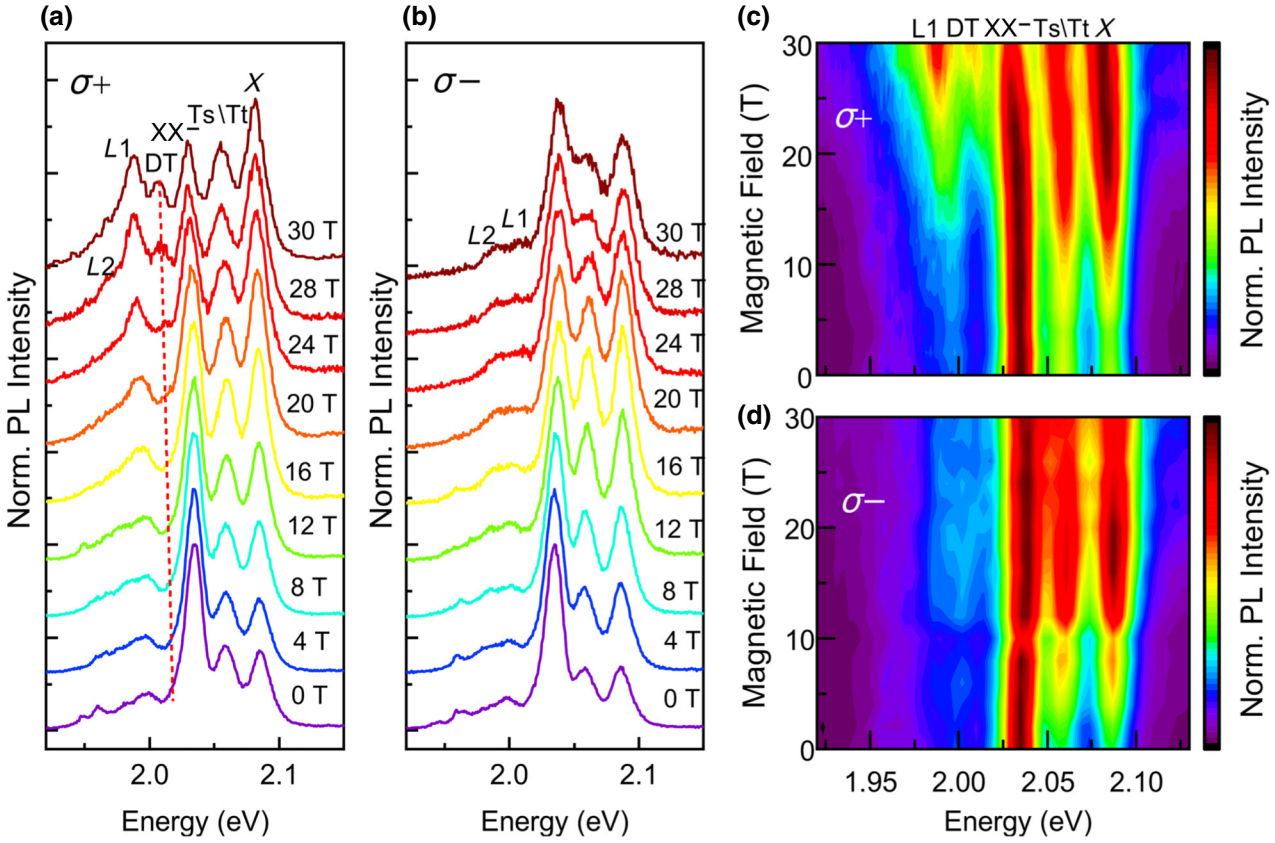

FIG. 3. PL spectra of the WS_2-talc ML sample at 4.2 K for σ^+ (a) and σ^- (b) detection, measured at position $P2$ and at different magnetic fields, using a laser power of 61 μW and circularly polarized excitation (σ^+). For clarity, spectra are vertically shifted. (c),(d) False color maps of the corresponding PL intensity as a function of magnetic field for, respectively, σ^+ and σ^- detection.

it is usually affected by different nonequilibrium phenomena, such as intervalley relaxation of carriers and spin-flip processes [16,31]. Therefore, further studies, including time-resolved PL and magneto-PL, are necessary to understand, in more detail, the magnetic field dependence of the trion's polarization degrees.

The polarization of the charged biexciton peak shows nonmonotonous behavior, increasing up to 10 T and subsequently decreasing until it reverses sign at the highest magnetic field. To further illustrate this behavior, Fig. S4 within Supplemental Material [25] shows the σ^-- and σ^+-polarized PL spectra for both the $P1$ and $P2$ positions for selected magnetic fields. At high fields (30 T), the σ^--polarized high-energy XX^- peak is brighter than its low-energy σ^+-polarized counterpart, even for the σ^+-laser excitation used here, which leads to an overall higher σ^+ PL intensity due to the induced valley polarization. This peculiar behavior was previously observed [5,33] and is related to the fact that the energy difference between the two Zeeman states of the biexciton is determined by the total g factor (g_t), including the contributions from all four constituent particles of the biexciton [34]. In contrast, the spectral difference between the σ^- and σ^+ PL peaks in an applied magnetic field is determined by the Zeeman states of the emitting bright exciton, given by the spectral g factor (g_s). The different values, and signs, of the total g-factor ($g_t \approx +4$) and the spectral g factor ($g_s \approx -4.3$), therefore, explain why the spectrally lower-energy emission peak corresponds to a higher-energy biexciton state that has a lower intensity than its higher-energy counterpart [5,34]. This effect is particularly evident when comparing the 30-T PL spectra obtained using parallel circular polarizations for excitation-detection (Fig. S5 within the Supplemental Material [25]), removing the effect of the induced valley polarization present when comparing the intensities of σ^- and σ^+ PL under σ^+ excitation (Fig. S4 within the Supplemental Material [25]). The biexciton peak at 2.038 eV for σ^-,σ^- polarization has higher intensity than the biexciton peak at 2.030 eV for σ^+,σ^+ polarization, in contrast to the regular behavior observed for the neutral-exciton emission.

Finally, we observe a clear increase, with increasing magnetic field, of the PL intensity of the dark trions in σ^+ detection, resulting in a positive polarization degree. These results are obtained using systematic fitting of the spectra for both detected polarizations (results in Fig. S6 within the Supplemental Material [25]) at position $P2$. We

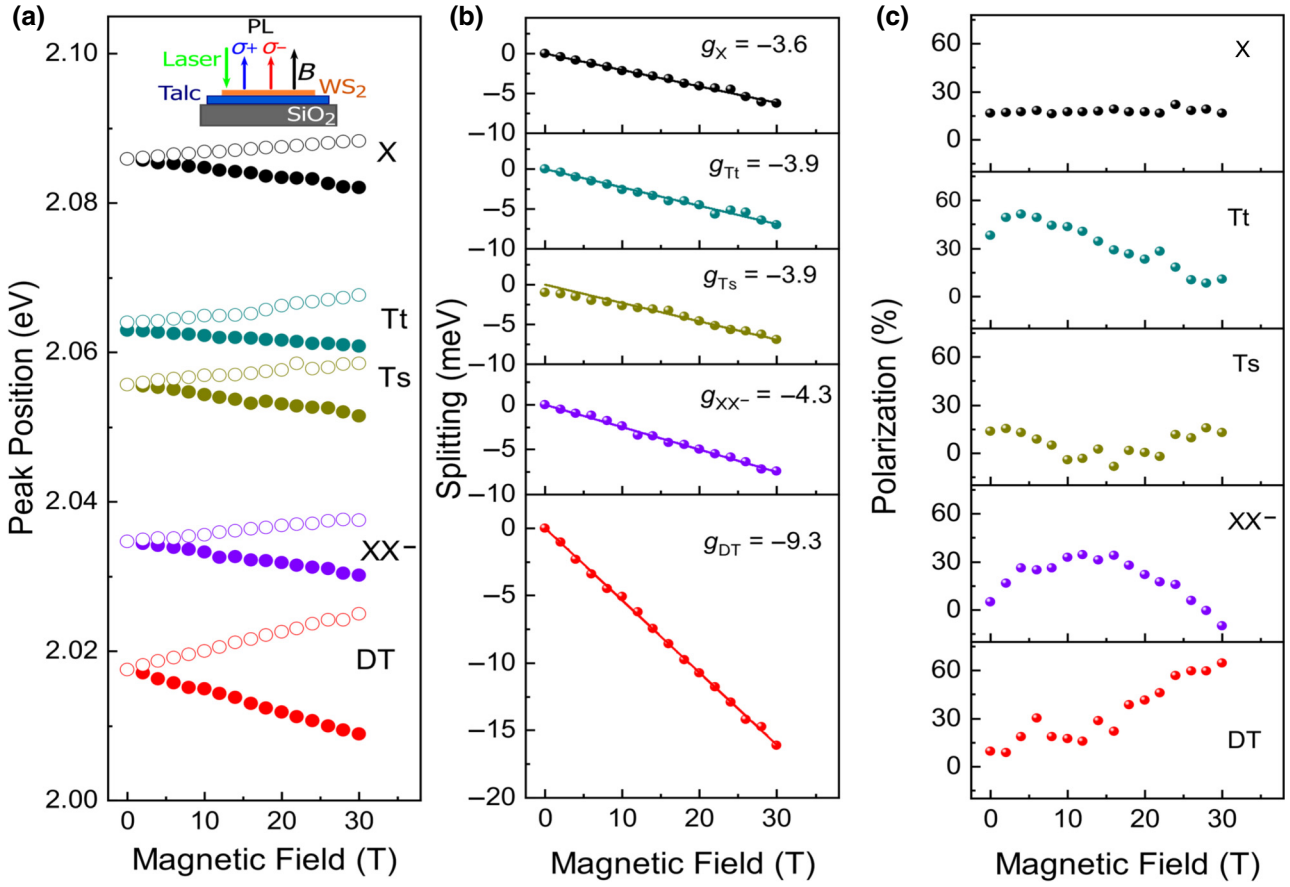

FIG. 4. (a) PL peak position versus magnetic field for σ^+ (filled circles) and σ^- detection (open circles) of all observed excitonic species. (b) Corresponding splittings of peaks versus magnetic field. (c) Corresponding polarization degrees as a function of magnetic field. All results are obtained at position $P2$ using circularly polarization excitation (σ^+).

note that at position $P1$ (Fig. S2 in Supplemental Material [26]) the DT emission is more visible than that for position $P2$, but for this position the DT emission peak can hardly be seen in σ^- detection due to the superposition of this peak with the XX^- emission peak. Previously, dark excitons and trions in monolayer WS_2 were observed in parallel or tilted magnetic fields [6,48], where the in-plane magnetic field brightens the dark-exciton and -trion emission due to the mixing of the spin components of the conduction bands [48]. We attribute the observation of the dark-trion emission in our experiments to the use of the high-numerical-aperture objective. The positive degree of circular polarization of the DT emission is related to the occurrence of intervalley scattering mechanisms, where the possibility to emit a photon is determined by the optically excited minority carrier (holes for n doping and electrons for hole doping) under weak optical excitation conditions [5]. Therefore, the PL of the negatively charged dark exciton is expected to exhibit the same valley polarization as that from X, whereas the positively charged dark exciton is expected to have opposite valley polarization relative to X [5]. For our sample, we observe the same polarization signs for the X and DT emissions, which indicates that monolayer WS_2 on talc is naturally n-doped, and its doping is not affected by the talc layer, which is consistent with our interpretation of the PL spectrum at zero magnetic field described above. This result is different from a previous study on graphene-talc [18], which has demonstrated a substrate-induced p doping of graphene-talc. The PL decay time of the DT emission is much longer than that of bright excitons and trions. Therefore, thermalization of the DT states occurs within their lifetime, resulting in an increasing DT polarization with increasing magnetic field, in contrast to the constant circular polarization of X and to previous studies of DTs in ML WSe_2 [47].

In addition, we also extract the g factors of the lower-energy emission peaks at 2.000 eV (labeled $L1$) and 1.982 eV (labeled $L2$). Figure S8 within the Supplemental Material [25] shows the magnetic field dependence of the PL peak positions for σ^+ and σ^- detection and the valley Zeeman splitting of these peaks. These lower-emission peaks follow selection rules similar to the bright-exciton emission, i.e., they show conservation of excitation

helicity in emission (circularly polarized emission). We obtain g factors of about -12.3 and -12.6 for the $L1$ and $L2$ emission peaks, respectively (Fig. S9 within the Supplemental Material [25]). We note that the energy separation of these peaks from the DT peak is about 17.8 meV for $L1$ and about 35.8 meV for $L2$. The nature of these peaks is not well established. Similar lower-emission peaks having similar g factors were recently reported for high-quality ML WS_2 and associated with a momentum-forbidden dark trion with the emission of optical (E'') or acoustic (ZA, LA) phonons, i.e., phonon replicas of dark trions [5]. The positions of the phonon replicas of the dark-trion emission are expected to be redshifted from the DT peak by the phonon energies of ML WS_2. Comparing the measured redshift (approximately 35.8 meV) and the theoretical phonon energy (36.4 meV) [12], the peak at about 1.982 eV ($L2$ peak) can be identified as a phonon-replica TD E'' (Γ). The shift of the $L1$ peak around 2.000 eV (approximately 17.8 meV) is close to the theoretical energy values of the $TA(K)$ and $ZA(K)$ phonons (18.2 and 17.7 meV) [12]. Furthermore, other phonon replicas, which could involve a momentum flip, can be induced by phonons from the K point. It would be possible to transfer an electron (hole) between K valleys with an emission of E'' (K) [$LA(K)$] phonons [12]. Their theoretical energies (43.0 and 22.6 meV) [12] are also close to the measured PL energy redshifts (35.8 and 17.8 meV) from the dark-trion peaks in our samples. Therefore, the observed $L1$ and $L2$ peaks can be associated with dark-trion replicas due to momentum-forbidden dark transitions. Particularly, the obtained g factors of $L1$ and $L2$ are consistent with previously reported values [2,6] for phonon replicas of dark-trion TD $ZA(K)$ and TD $E''(K)$, respectively.

IV. CONCLUSION

We investigate the low-temperature photoluminescence and magnetophotoluminescence of monolayer WS_2 on talc. We obtain high-quality samples showing the emission of different excitonic complexes in the PL spectra at low temperatures. At low temperature, we observe that the FWHM of the exciton peak is comparable to that of WS_2/h-BN, showing that talc is a promising dielectric to separate monolayer TMD from the SiO_2 substrate. We investigate the properties of all excitonic complexes under perpendicular magnetic fields up to 30 T and extract the g factor of all emission peaks. The obtained g factors are in agreement with theoretical values reported in the literature [12]. In contrast to previous studies of graphene and talc [18], which demonstrate spontaneous p doping, our magneto-PL results indicate that ML WS_2-talc is naturally n-doped, as revealed by the observation of the same valley polarization for the X and charged DT emissions. One possible explanation for this result is that p doping from talc could result in a reduction of the n doping of ML WS_2, but it is not enough to affect the type of doping. In addition, we observe that, under σ^+-polarized excitation, the sign of circularly polarization biexcitons is reversed under higher magnetic fields, which shows that under very high fields the effect of thermalization is the dominant mechanism, compared with valley selectivity. We also observe that the polarization of the dark-trion emission increases considerably with increasing magnetic field, in contrast to previous studies on ML WSe_2. In general, the improvement of the optical quality of TMD on talc dielectric also contributes to uncovering further information on the valley physics of ML WS_2, particularly for the properties of biexcitons and dark trions under high perpendicular magnetic fields. Finally, our results suggest that talc is a promising low-cost layered material to explore fundamental physics and for possible application in optoelectronic devices based on high-quality doped TMD heterostructures.

ACKNOWLEDGMENTS

The work is supported by the Fundação de Amparo a Pesquisa do Estado de São Paulo (Fapesp) (Grants No. 18/01808-5 and No. 19/23488-5); the Conselho Nacional de Desenvolvimento Científico e Tecnológico (CNPQ) (Grants No. 426634/2018-7 and No. 311678/2020-3); and the High-Field Magnet Laboratory (HFML-RU/NWO-I), a member of the European Magnetic Field Laboratory (EMFL). G.P. acknowledges the "Coordenação de Aperfeiçoamento de Pessoal de Nível Superior" (Capes) for financial support of her PhD. I.D.B. acknowledges financial support from the Brazilian Nanocarbon Institute of Science and Technology (INCT/Nanocarbono), the Brazilian Synchrotron Light Laboratory (LNLS), Fapesp (Grant NO. 2018/00823-0), CNPq (Grant No. 311327/2020-6), and L'ORÉAL-UNESCO-ABC for Women in Science Brazil 2021. We would like to acknowledge F. Iikawa and O.D.D. Couto, Jr. for preliminarily optical characterization of our samples, and J. Buhot and M. Ballottin for optical alignment of the magneto-PL setup. The authors also would like to acknowledge the IMBUIA beamline at the Brazilian Synchrotron Light Laboratory (LNLS) for the AFM facility.

[1] G. Wang, A. Chernikov, M. M. Glazov, T. F. Heinz, X. Marie, T. Amand, and B. Urbaszek, Colloquium: Excitons in atomically thin transition metal dichalcogenides, Rev. Mod. Phys. **90**, 21001 (2018).

[2] T. Mueller and E. Malic, Exciton physics and device application of Two-dimensional transition metal dichalcogenide semiconductors, npj 2D Mater. Appl. **2**, 29 (2018).

[3] K. F. Mak and J. Shan, Photonics and optoelectronics of 2D semiconductor transition metal dichalcogenides, Nat. Photonics **10**, 216 (2016).

[4] F. Cadiz, E. Courtade, C. Robert, G. Wang, Y. Shen, H. Cai, T. Taniguchi, K. Watanabe, H. Carrere, D. Lagarde, M. Manca, T. Amand, P. Renucci, S. Tongay, X. Marie, and B. Urbaszek, Excitonic Linewidth Approaching the Homogeneous Limit in MoS_2-Based van der Waals Heterostructures, Phys. Rev. X **7**, 021026 (2017).

[5] Z. Li, T. Wang, S. Miao, Z. Lian, and S. F. Shi, Fine structures of valley-polarized excitonic states in monolayer transitional metal dichalcogenides, Nanophotonics **9**, 1811 (2020).

[6] M. Zinkiewicz, A. O. Slobodeniuk, T. Kazimierczuk, P. Kapuściński, K. Oreszczuk, M. Grzeszczyk, M. Bartos, K. Nogajewski, K. Watanabe, T. Taniguchi, C. Faugeras, P. Kossacki, M. Potemski, A. Babiński, and M. R. Molas, Neutral and charged dark excitons in monolayer WS_2, Nanoscale **12**, 18153 (2020).

[7] G. Wang, C. Robert, M. M. Glazov, F. Cadiz, E. Courtade, T. Amand, D. Lagarde, T. Taniguchi, K. Watanabe, B. Urbaszek, and X. Marie, In-Plane Propagation of Light in Transition Metal Dichalcogenide Monolayers: Optical Selection Rules, Phys. Rev. Lett. **119**, 47401 (2017).

[8] H. Zeng, J. Dai, W. Yao, D. Xiao, and X. Cui, Valley polarization in MoS_2 monolayers by optical pumping, Nat. Nanotechnol. **7**, 490 (2012).

[9] G. Plechinger, P. Nagler, J. Kraus, N. Paradiso, C. Strunk, C. Schüller, and T. Korn, Identification of excitons, trions and biexcitons in single-layer WS_2, Phys. Status Solidi RRL **9**, 457 (2015).

[10] A. Steinhoff, M. Florian, A. Singh, K. Tran, M. Kolarczik, S. Helmrich, A. W. Achtstein, U. Woggon, N. Owschimikow, F. Jahnke, and X. Li, Biexciton fine structure in monolayer transition metal dichalcogenides, Nat. Phys. **14**, 1199 (2018).

[11] E. Mostaani, M. Szyniszewski, C. H. Price, R. Maezono, M. Danovich, R. J. Hunt, N. D. Drummond, and V. I. Fal'Ko, Diffusion quantum monte carlo study of excitonic complexes in Two-dimensional transition-metal dichalcogenides, Phys. Rev. B **96**, 075431 (2017).

[12] M. Zinkiewicz, T. Woźniak, T. Kazimierczuk, P. Kapuscinski, K. Oreszczuk, M. Grzeszczyk, M. Bartoš, K. Nogajewski, K. Watanabe, T. Taniguchi, C. Faugeras, P. Kossacki, M. Potemski, A. Babiński, and M. R. Molas, Excitonic complexes in n-doped WS_2 monolayer, Nano Lett. **6**, 2519 (2021).

[13] M. Danovich, V. Zólyomi, and V. I. Fal'Ko, Dark trions and biexcitons in WS_2 and WSe_2 made bright by e-e scattering, Sci. Rep. **7**, 45998 (2017).

[14] Z. Li, T. Wang, C. Jin, Z. Lu, Z. Lian, Y. Meng, M. Blei, S. Gao, T. Taniguchi, K. Watanabe, T. Ren, S. Tongay, L. Yang, D. Smirnov, T. Cao, and S. F. Shi, Emerging photoluminescence from the dark-exciton phonon replica in monolayer WSe_2, Nat. Commun. **10**, 2469 (2019).

[15] A. Arora, N. K. Wessling, T. Deilmann, T. Reichenauer, P. Steeger, P. Kossacki, M. Potemski, S. Michaelis De Vasconcellos, M. Rohlfing, and R. Bratschitsch, Dark trions govern the temperature-dependent optical absorption and emission of doped atomically thin semiconductors, Phys. Rev. B **101**, 241413(R) (2020).

[16] A. Arora, Magneto-optics of layered Two-dimensional semiconductors and heterostructures: Progress and prospects, J. Appl. Phys. **129**, 120902 (2021).

[17] A. B. Alencar, A. P. M. Barboza, B. S. Archanjo, H. Chacham, and B. R. A. Neves, Experimental and theoretical investigations of monolayer and Few-layer talc, 2D Mater. **2**, 015004 (2015).

[18] E. Mania, A. B. Alencar, A. R. Cadore, B. R. Carvalho, K. Watanabe, T. Taniguchi, B. R. A. Neves, H. Chacham, and L. C. Campos, Spontaneous doping on high quality talc-graphene-hBN van der waals heterostructures, 2D Mater. **4**, 031008 (2017).

[19] J. L. Rosenholtz and D. T. Smith, The dielectric constant of mineral powders, Am. Mineral. J. Earth Planet. Mater. **21**, 115 (1936). http://www.minsocam.org/msa/collectors_corner/amtoc/toc1936.htm

[20] I. D. Barcelos, A. R. Cadore, A. B. Alencar, F. C. B. Maia, E. Mania, R. F. Oliveira, C. C. B. Bufon, Â Malachias, R. O. Freitas, R. L. Moreira, and H. Chacham, Infrared fingerprints of natural 2D talc and plasmon–phonon coupling in graphene–talc heterostructures, ACS Photonics **5**, 1912 (2018).

[21] A. C. Gadelha, T. L. Vasconcelos, L. G. Cançado, and A. Jorio, Nano-optical imaging of In-plane homojunctions in graphene and MoS_2 van der waals heterostructures on talc and SiO_2, J. Phys. Chem. Lett. **12**, 7625 (2021).

[22] D. Nutting, G. A. Prando, M. Severijnen, I. Barcelos, S. Guo, P. C. M. Christianen, U. Zeitler, Y. Galvão Gobato, and F. Withers, Electrical and optical properties of transition metal dichalcogenides on talc dielectrics, Nanoscale **13**, 15853 (2021).

[23] E. Liu, J. Van Baren, C. T. Liang, T. Taniguchi, K. Watanabe, N. M. Gabor, Y. C. Chang, and C. H. Lui, Multipath Optical Recombination of Intervalley Dark Excitons and Trions in Monolayer WSe_2, Phys. Rev. Lett. **124**, 196802 (2020).

[24] V. Orsi Gordo, M. A. G. Balanta, Y. Galvão Gobato, F. S. Covre, H. V. A. Galeti, F. Iikawa, O. D. D. Couto, F. Qu, M. Henini, D. W. Hewak, and C. C. Huang, Revealing the nature of Low-temperature photoluminescence peaks by laser treatment in van der waals epitaxially grown WS_2 monolayers, Nanoscale **10**, 4807 (2018).

[25] See the Supplemental Material at http://link.aps.org/supplemental/10.1103/PhysRevApplied.16.064055 for details of AFM images and PL spectra.

[26] G. Plechinger, P. Nagler, A. Arora, R. Schmidt, A. Chernikov, A. G. Del Águila, P. C. M. Christianen, R. Bratschitsch, C. Schüller, and T. Korn, Trion fine structure and coupled spin–valley dynamics in monolayer tungsten disulfide, Nat. Commun. **7**, 12715 (2016).

[27] I. Paradisanos, K. M. McCreary, D. Adinehloo, L. Mouchliadis, J. T. Robinson, H. J. Chuang, A. T. Hanbicki, V. Perebeinos, B. T. Jonker, E. Stratakis, and G. Kioseoglou, Prominent room temperature valley polarization in WS_2/graphene heterostructures grown by chemical vapor deposition, Appl. Phys. Lett. **116**, 203102 (2020).

[28] J. Jadczak, L. Bryja, J. Kutrowska-Girzycka, P. Kapuściński, M. Bieniek, Y. S. Huang, and P. Hawrylak, Room temperature multi-phonon upconversion photoluminescence in monolayer semiconductor WS_2, Nat. Commun. **10**, 107 (2019).

[29] Y. Liu, C. Liu, Z. Ma, G. Zheng, Y. Ma, and Z. Sheng, Annealing effect on photoluminescence of Two

dimensional WSe_2/BN heterostructure, Appl. Phys. Lett. **117**, 233103 (2020).

[30] T. P. Lyons, S. Dufferwiel, M. Brooks, F. Withers, T. Taniguchi, K. Watanabe, K. S. Novoselov, G. Burkard, and A. I. Tartakovskii, The calley zeeman effect in inter- and intra-valley trions in monolayer WSe_2, Nat. Commun. **10**, 2330 (2019).

[31] P. Kapuściński, D. Vaclavkova, M. Grzeszczyk, A. O. Slobodeniuk, K. Nogajewski, M. Bartos, K. Watanabe, T. Taniguchi, C. Faugeras, A. Babiński, M. Potemski, and M. R. Molas, Valley polarization of singlet and triplet trions in a WS_2 monolayer in magnetic fields, Phys. Chem. Chem. Phys. **22**, 19155 (2020).

[32] D. Vaclavkova, J. Wyzula, K. Nogajewski, M. Bartos, A. O. Slobodeniuk, C. Faugeras, M. Potemski, and M. R. Molas, Singlet and triplet trions in WS_2 monolayer encapsulated in hexagonal boron nitride, Nanotechnology **29**, 325705 (2019).

[33] P. Nagler, M. V. Ballottin, A. A. Mitioglu, M. V. Durnev, T. Taniguchi, K. Watanabe, A. Chernikov, C. Schüller, M. M. Glazov, P. C. M. Christianen, and T. Korn, Zeeman Splitting and Inverted Polarization of Biexciton Emission in Monolayer WS_2, Phys. Rev. Lett. **121**, 57402 (2018).

[34] Z. Li, T. Wang, Z. Lu, C. Jin, Y. Chen, Y. Meng, Z. Lian, T. Taniguchi, K. Watanabe, S. Zhang, D. Smirnov, and S.-F. Shi, Revealing the biexciton and trion-exciton complexes in BN encapsulated WSe_2, Nat. Commun. **9**, 3719 (2018).

[35] M. Barbone, A. R. P. Montblanch, D. M. Kara, C. Palacios-Berraquero, A. R. Cadore, D. De Fazio, B. Pingault, E. Mostaani, H. Li, B. Chen, K. Watanabe, T. Taniguchi, S. Tongay, G. Wang, A. C. Ferrari, and M. Atatüre, Charge-tuneable biexciton complexes in monolayer WSe_2, Nat. Commun. **9**, 3721 (2018).

[36] C. Robert, When bright and dark bind together, Nat. Nanotechnol. **13**, 982 (2018).

[37] Y. You, X. X. Zhang, T. C. Berkelbach, M. S. Hybertsen, D. R. Reichman, and T. F. Heinz, Observation of biexcitons in monolayer WSe_2, Nat. Phys. **11**, 477 (2015).

[38] M. He, P. Rivera, D. Van Tuan, N. P. Wilson, M. Yang, T. Taniguchi, K. Watanabe, J. Yan, D. G. Mandrus, H. Yu, H. Dery, W. Yao, and X. Xu, Valley phonons and exciton complexes in a monolayer semiconductor, Nat. Commun. **11**, 618 (2020).

[39] G. Aivazian, Z. Gong, A. M. Jones, R. L. Chu, J. Yan, D. G. Mandrus, C. Zhang, D. Cobden, W. Yao, and X. Xu, Magnetic control of valley pseudospin in monolayer WSe_2, Nat. Phys. **11**, 148 (2015).

[40] Y. Li, J. Ludwig, T. Low, A. Chernikov, X. Cui, G. Arefe, Y. D. Kim, A. M. Van Der Zande, A. Rigosi, H. M. Hill, S. H. Kim, J. Hone, Z. Li, D. Smirnov, and T. F. Heinz, Valley Splitting and Polarization by the Zeeman Effect in Monolayer $MoSe_2$, Phys. Rev. Lett. **113**, 266804 (2014).

[41] A. Srivastava, M. Sidler, A. V. Allain, D. S. Lembke, A. Kis, and A. Imamoglu, Valley zeeman effect in elementary optical excitations of monolayer WSe_2, Nat. Phys. **11**, 141 (2015).

[42] D. Macneill, C. Heikes, K. F. Mak, Z. Anderson, A. Kormányos, V. Zólyomi, J. Park, and D. C. Ralph, Breaking of Valley Degeneracy by Magnetic Field in Monolayer $MoSe_2$, Phys. Rev. Lett. **114**, 037401 (2015).

[43] G. Wang, L. Bouet, M. M. Glazov, T. Amand, E. L. Ivchenko, E. Palleau, X. Marie, and B. Urbaszek, Magneto-Optics in transition metal diselenide monolayers, 2D Mater. **2**, 34002 (2015).

[44] A. V. Stier, K. M. McCreary, B. T. Jonker, J. Kono, and S. A. Crooker, Exciton diamagnetic shifts and valley zeeman effects in monolayer WS_2 and MoS_2 to 65 tesla, Nat. Commun. **7**, 10643 (2016).

[45] G. Plechinger, P. Nagler, A. Arora, A. Granados Del Águila, M. V. Ballottin, T. Frank, P. Steinleitner, M. Gmitra, J. Fabian, P. C. M. Christianen, R. Bratschitsch, C. Schüller, and T. Korn, Excitonic valley effects in monolayer WS_2 under high magnetic fields, Nano Lett. **16**, 7899 (2016).

[46] M. Goryca, J. Li, A. V. Stier, T. Taniguchi, K. Watanabe, E. Courtade, S. Shree, C. Robert, B. Urbaszek, X. Marie, and S. A. Crooker, Revealing exciton masses and dielectric properties of monolayer semiconductors with high magnetic fields, Nat. Commun. **10**, 4172 (2019).

[47] Z. Li, T. Wang, Z. Lu, M. Khatoniar, Z. Lian, Y. Meng, M. Blei, T. Taniguchi, K. Watanabe, S. A. McGill, S. Tongay, V. M. Menon, D. Smirnov, and S. F. Shi, Direct observation of gate-tunable dark trions in monolayer WSe_2, Nano Lett. **19**, 6886 (2019).

[48] C. Robert, B. Han, P. Kapuscinski, A. Delhomme, C. Faugeras, T. Amand, M. R. Molas, M. Bartos, K. Watanabe, T. Taniguchi, B. Urbaszek, M. Potemski, and X. Marie, Measurement of the spin-forbidden dark excitons in MoS_2 and $MoSe_2$ monolayers, Nat. Commun. **11**, 4037 (2020).